

Skin values of ^{208}Pb and ^{48}Ca determined from reaction cross sections

Tomotsugu Wakasa, Shingo Tagami, and Masanobu Yahiro*
Department of Physics, Kyushu University, Fukuoka 819-0395, Japan

Background: The PREX and the CREX group reported skin values, $r_{\text{skin}}^{208}(\text{PREX2}) = 0.283 \pm 0.071 \text{ fm}$ and $r_{\text{skin}}^{48}(\text{CREX}) = 0.121 \pm 0.026 \text{ (exp)} \pm 0.024 \text{ (model) fm}$, respectively. Using the Love-Franey (LF) t -matrix folding model with the neutron and proton densities scaled to the neutron radius $r_n^{208}(\text{PREX2})$ and the proton radius of the electron scattering, we found that the reaction cross sections σ_R reproduce the data for $p + ^{208}\text{Pb}$ scattering at $E_{\text{lab}} = 534.1, 549, 806 \text{ MeV}$. Zenihiro *et al.* deduce neutron radii $r_n^{48,40}(\text{exp})$ from the angular distributions of the cross sections and analyzing powers of proton elastic scattering, whereas we determine matter radius $r_m^{40}(\text{exp}) = 3.361 \pm 0.075 \text{ fm}$ from measured σ_R for $^4\text{He} + ^{40}\text{Ca}$ scattering.

Aim: Our first aim is to determine r_{skin}^{208} from measured σ_R of $p + ^{208}\text{Pb}$ scattering at $E_{\text{lab}} = 534.1, 549, 806 \text{ MeV}$ by using the Love-Franey (LF) t -matrix folding model. Our second aim is to determine r_{skin}^{48} from the $r_m^{40}(\text{exp})$ and the difference $\Delta \equiv r_m^{48}(\text{exp}) - r_m^{40}(\text{exp})$ that is evaluated from the $r_n^{48,40}(\text{exp})$ and the $r_p^{48,40}(\text{exp})$ calculated with the isotope shift method based on the electron scattering.

Method and results: For the first aim, we use the Love-Franey t -matrix model with the densities scaled from the D1S-GHFB+AMP neutron density, where D1S-GHFB+AMP stands for D1S Gogny HFB (GHFB) with the angular momentum projection (AMP). The D1M-GHFB+AMP is also used to estimate a theoretical error. The resulting skin values are $r_{\text{skin}}^{208} = 0.324 \pm 0.047 \text{ fm}$ for D1S and $r_{\text{skin}}^{208}(\text{exp}) = 0.333 \pm 0.047 \text{ fm}$ for D1M. The difference $\Delta = 0.109 \text{ fm}$ and $r_m^{40}(\text{exp}) = 3.361 \pm 0.075 \text{ fm}$ yield $r_m^{48} = 3.470 \pm 0.075 \text{ fm}$, leading to $r_{\text{skin}}^{48} = 0.144 \pm 0.075 \text{ fm}$.

Conclusion: We conclude that $r_{\text{skin}}^{208}(\text{exp}) = 0.324 \pm (0.047)_{\text{exp}} \pm (0.009)_{\text{th}} \text{ fm}$ for p scattering at $E_{\text{lab}} = 534.1, 549, 806 \text{ MeV}$. Our skin value $r_{\text{skin}}^{48} = 0.144 \pm 0.083 = 0.061 \sim 0.227 \text{ fm}$ is consistent with $r_{\text{skin}}^{48}(\text{CREX}) = 0.071 \sim 0.171 \text{ fm}$.

Background: Horowitz *et al.* [1] proposed a direct measurement for neutron skin r_{skin} . The measurement consists of parity-violating weak scattering and elastic electron scattering. The neutron radius r_n is determined from the former experiment, whereas the proton radius r_p is from the latter.

The direct measurement was applied for ^{208}Pb and ^{48}Ca . As for ^{208}Pb , the PREX collaboration presented

$$r_{\text{skin}}^{208}(\text{PREX2}) = 0.283 \pm 0.071 \text{ fm}, \quad (1)$$

combining the original Lead Radius EXperiment (PREX) result with the updated PREX2 result [2–4]. As for ^{48}Ca , the CREX group presented [5]

$$\begin{aligned} r_{\text{skin}}^{48}(\text{CREX}) &= 0.121 \pm 0.026 \text{ (exp)} \pm 0.024 \text{ (model)} \\ &= 0.071 \sim 0.171 \text{ fm}. \end{aligned} \quad (2)$$

The $r_{\text{skin}}^{208}(\text{PREX2})$ and the $r_{\text{skin}}^{48}(\text{CREX})$ are most reliable at the present stage, and provide crucial tests for the equation of state (EoS) of nuclear matter [6–10] as well as nuclear structure.

Reed *et al.* [11] reported a value of the slope parameter of the EoS and examine the impact of such a stiff symmetry energy on some critical neutron-star observables. The $r_{\text{skin}}^{208}(\text{PREX2})$ value is considerably larger than the other experimental values that are model-dependent [12–15]. Meanwhile, the nonlocal dispersive-optical-model (DOM) analysis of ^{208}Pb yields $r_{\text{skin}}^{\text{DOM}} = 0.25 \pm 0.05 \text{ fm}$ [16]. The value is consistent with $r_{\text{skin}}^{208}(\text{PREX2})$.

Using the chiral (Kyushu) g -matrix folding model, we determine $r_{\text{skin}}^{208}(\text{exp}) = 0.278 \pm 0.035 \text{ fm}$ from reaction cross

section σ_R in $30 \leq E_{\text{lab}} \leq 100 \text{ MeV}$ [17]. In addition, for $^4\text{He} + ^{208}\text{Pb}$ scattering, we determine $r_{\text{skin}}^{208}(\text{exp}) = 0.416 \pm 0.146 \text{ fm}$ from measured σ_R in $E_{\text{lab}} = 30 \sim 50 \text{ MeV}$ [18]. These values are consistent with $r_{\text{skin}}^{208}(\text{PREX2})$.

For ^{12}C scattering on ^9Be , ^{12}C , ^{27}Al targets, we tested reliability of the Kyushu g -matrix folding model and found that the folding model is reliable in $30 \leq E_{\text{lab}} \leq 100 \text{ MeV}$ and $250 \leq E_{\text{lab}} \leq 400 \text{ MeV}$ [19]. Furthermore, we mentioned that the difference between the t -matrix and the g -matrix is small in $E_{\text{lab}} \gtrsim 400 \text{ MeV}$. Since the cutoff of the chiral nucleon-nucleon (NN) is 550 MeV, the chiral NN t -matrix is useful in $400 \leq E_{\text{lab}} \leq 500 \text{ MeV}$. For $E_{\text{lab}} \gtrsim 400 \text{ MeV}$, the most famous t -matrix is Love-Franey (LF) t -matrix [20].

As for ^{208}Pb , it is possible to determine reliable neutron radius $r_n(\text{PREX2}) = 5.727 \pm 0.071 \text{ fm}$ and matter radius $r_m(\text{PREX2}) = 5.617 \pm 0.044 \text{ fm}$ from $r_p(\text{exp}) = 5.444 \text{ fm}$ [21] of electron scattering and $r_{\text{skin}}^{208}(\text{PREX2})$. The r_p calculated with D1S-Gogny-HFB (D1S-GHFB) with the angular momentum projection (AMP) agrees with $r_p(\text{exp})$. The neutron density calculated with D1S-GHFB+AMP is scaled so as to $r_n^{\text{scaling}} = 5.727 \text{ fm}$. In Ref. [22], we showed that the LF t -matrix folding model with the scaled neutron density and the D1S-GHFB+AMP proton one reproduces the data $\sigma_R(\text{exp})$ [23, 24] at $E_{\text{lab}} = 534.1, 549, 806 \text{ MeV}$ within total error bars. Nevertheless, we do not determine r_{skin}^{208} from the data at $E_{\text{lab}} = 534.1, 549, 806 \text{ MeV}$.

As for ^{48}Ca , an indirect measurement is made with the high-resolution $E1$ polarizability experiment (E1pE) [25]. The skin value $r_{\text{skin}}^{48}(E1\text{pE}) = 0.14 \sim 0.20 \text{ fm}$ is consistent with $r_{\text{skin}}^{48}(\text{CREX})$. Using $^4\text{He} + ^{40}\text{Ca}$ scattering in $E_{\text{lab}} = 30 \sim 50 \text{ MeV}$, we determine matter radius $r_m^{40}(\text{exp})$ from measured σ_R [18], whereas Zenihiro *et al.* deduce neutron radii $r_n^{48,40}(\text{exp})$ from the angular distributions of the cross sections and analyzing powers of polarized proton elas-

* orion093g@gmail.com

tic scattering at $E_{\text{lab}} = 295$ MeV [26]. The $r_{\text{skin}}^{48}(\text{exp}) = 0.168_{-0.028}^{+0.025}$ fm determined by Zenihiro *et al.* is consistent with r_{skin}^{48} (CREX).

Aim: The first aim is to determine $r_{\text{skin}}^{208}(\text{exp})$ from the data [23, 24] on σ_R of $p + {}^{208}\text{Pb}$ scattering at $E_{\text{lab}} = 534.1, 549, 806$ MeV by using the LF t -matrix folding model.

The second aim is to determine $r_{\text{skin}}^{48}(\text{exp})$ with the result $r_m^{40}(\text{exp}) = 3.361 \pm 0.075$ fm [18] of ${}^4\text{He} + {}^{40}\text{Ca}$ scattering in $E_{\text{lab}} = 30 \sim 50$ MeV and the difference $\Delta \equiv r_m^{48}(\text{exp}) - r_m^{40}(\text{exp})$, since there is no data on σ_R for ${}^4\text{He} + {}^{48}\text{Ca}$ scattering. The derivation of Δ is shown below.

Method for determining $r_{\text{skin}}^{48}(\text{exp})$: Zenihiro *et al.* determine neutron radii $r_n^{40}(\text{exp}) = 3.375_{-0.023}^{+0.022}$ fm and $r_n^{48}(\text{exp}) = 3.555_{-0.028}^{+0.025}$ fm from the angular distributions of the cross sections and the analyzing powers of proton elastic scattering [26]. We can obtain the proton radii for ${}^{40,48}\text{Ca}$ with the isotope shift method based on the electron scattering [27], i.e., $r_p^{40}(\text{exp}) = 3.378$ fm and $r_p^{48}(\text{exp}) = 3.385$ fm. Using these values, we can obtain $r_m^{40}(\text{exp}) = 3.377_{-0.023}^{+0.022}$ fm, $r_m^{48}(\text{exp}) = 3.485_{-0.028}^{+0.025}$ fm.

From the central values of $r_m^{40}(\text{exp})$ and $r_m^{48}(\text{exp})$, we obtain the difference $\Delta \equiv r_m^{48}(\text{exp}) - r_m^{40}(\text{exp}) = 0.109$ fm. In Ref. [18], meanwhile, we determined $r_m^{40}(\text{exp}) = 3.361 \pm 0.075$ fm from measured σ_R of ${}^4\text{He} + {}^{40}\text{Ca}$ scattering in $E_{\text{lab}} = 30 \sim 50$ MeV. We can then obtain $r_m^{48}(\text{exp}) = 3.470 \pm 0.075$ fm from $r_m^{40}(\text{exp}) = 3.361 \pm 0.075$ fm and Δ . The $r_m^{48}(\text{exp}) = 3.470 \pm 0.075$ fm and $r_p^{48}(\text{exp}) = 3.385$ fm lead to $r_{\text{skin}}^{48}(\text{exp}) = 0.144 \pm 0.075$ fm, respectively.

Method for determining $r_{\text{skin}}^{208}(\text{exp})$: We use the folding model based on Lovey-dovey (LF) t -matrix [20] to determine $r_{\text{skin}}^{208}(\text{exp})$ from data $\sigma_R(\text{exp})$ [23, 24] at $E_{\text{lab}} = 534.1, 549, 806$ MeV. We have already applied the LF t -matrix folding model for $p + {}^{4,6,8}\text{He}$ scattering at 700 MeV to determine matter radii $r_m(\text{exp})$ from the high-accuracy data [28]. The results are $r_m(\text{exp}) = 2.48(3), 2.53(2)$ fm and $r_{\text{skin}} = 0.78(3), 0.82(2)$ fm for ${}^{6,8}\text{He}$ [29].

Now we show the formulation on the LF t -matrix folding model below. For proton-nucleus scattering, the potential $U(\mathbf{R})$ between an incident proton (p) and a target (T) has the direct and exchange parts, U^{DR} and U^{EX} , as

$$U^{\text{DR}}(\mathbf{R}) = \sum_{\mu, \nu} \int \rho_T^\nu(\mathbf{r}_T) t_{\mu\nu}^{\text{DR}}(s; \rho_{\mu\nu}) d\mathbf{r}_T, \quad (3a)$$

$$U^{\text{EX}}(\mathbf{R}) = \sum_{\mu, \nu} \int \rho_T^\nu(\mathbf{r}_T, \mathbf{r}_T + \mathbf{s}) \times t_{\mu\nu}^{\text{EX}}(s; \rho_{\mu\nu}) \exp[-i\mathbf{K}(\mathbf{R}) \cdot \mathbf{s}/M] d\mathbf{r}_T \quad (3b)$$

where \mathbf{R} is the relative coordinate between p and T, $\mathbf{s} = -\mathbf{r}_T + \mathbf{R}$, and \mathbf{r}_T is the coordinate of the interacting nucleon from T. Each of μ and ν denotes the z-component of isospin. The non-local U^{EX} has been localized in Eq. (3b) with the local semi-classical approximation [30–32] where $\mathbf{K}(\mathbf{R})$ is the local momentum between p and T, and $M = A/(1+A)$ for the mass number A of T; see Ref. [33] for the validity of the localization.

The direct and exchange parts, $t_{\mu\nu}^{\text{DR}}$ and $t_{\mu\nu}^{\text{EX}}$, of the t matrix

are described by

$$t_{\mu\nu}^{\text{DR}}(s) = \frac{1}{4} \sum_S \hat{S}^2 t_{\mu\nu}^{S1}(s) \text{ for } \mu + \nu = \pm 1, \quad (4)$$

$$t_{\mu\nu}^{\text{DR}}(s) = \frac{1}{8} \sum_{S,T} \hat{S}^2 t_{\mu\nu}^{ST}(s) \text{ for } \mu + \nu = 0, \quad (5)$$

$$t_{\mu\nu}^{\text{EX}}(s) = \frac{1}{4} \sum_S (-1)^{S+1} \hat{S}^2 t_{\mu\nu}^{S1}(s) \text{ for } \mu + \nu = \pm 1, \quad (6)$$

$$t_{\mu\nu}^{\text{EX}}(s) = \frac{1}{8} \sum_{S,T} (-1)^{S+T} \hat{S}^2 t_{\mu\nu}^{ST}(s) \text{ for } \mu + \nu = 0, \quad (7)$$

where $\hat{S} = \sqrt{2S+1}$ and $t_{\mu\nu}^{ST}$ are the spin-isospin components of the t -matrix interaction.

As proton and neutron densities, $\rho_T^{\nu=-1/2}$ and $\rho_T^{\nu=1/2}$, we use D1S-GHFB+AMP; see Ref. [34] for the formulation. As a way of taking the center-of-mass correction to the densities, we adapt the method of Ref. [35].

We scale the D1S-GHFB+AMP neutron density so that the radius $r_n(\text{scaling})$ of the scaled density can reproduce $\sigma_R(\text{exp})$, since the r_p calculated with the D1S-GHFB+AMP density agrees with $r_p^{\text{exp}} = 5.444$ fm [21] of electron scaling. The same procedure is taken the D1M-GHFB+AMP neutron density, where D1M [36, 37] is an improved version of D1S and the proton radius calculated with D1M-GHFB+AMP agrees with $r_p^{\text{exp}} = 5.444$ fm.

Our scaling procedure is explained below. The scaled density $\rho_{\text{scaling}}(\mathbf{r})$ is determined from the original (D1S-GHFB+AMP or D1M-GHFB+AMP) one $\rho(\mathbf{r})$ as

$$\rho_{\text{scaling}}(\mathbf{r}) \equiv \frac{1}{\alpha^3} \rho(\mathbf{r}/\alpha), \quad \mathbf{r}_{\text{scaling}} \equiv \mathbf{r}/\alpha \quad (8)$$

with a scaling factor

$$\alpha = \sqrt{\frac{\langle \mathbf{r}^2 \rangle_{\text{scaling}}}{\langle \mathbf{r}^2 \rangle}}. \quad (9)$$

In Eq. (8), we have replaced \mathbf{r} by \mathbf{r}/α in the original density. Eventually, \mathbf{r} dependence of $\rho_{\text{scaling}}(\mathbf{r})$ is different from that of $\rho(\mathbf{r})$. We have multiplied the original density by α^{-3} in order to normalize the scaled density. The symbol means $\sqrt{\langle \mathbf{r}^2 \rangle_{\text{scaling}}}$ is the root-mean-square radius of $\rho_{\text{scaling}}(\mathbf{r})$.

Results for $r_{\text{skin}}^{208}(\text{exp})$: Figure 1 shows σ_R as a function of E_{lab} . The results of D1S-GHFB+AMP and D1M-GHFB+AMP are near the lower bound of data [23, 24] in $500 \leq E_{\text{lab}} \leq 900$ MeV. The result of D1S-GHFB+AMP is better than that of D1M-GHFB+AMP.

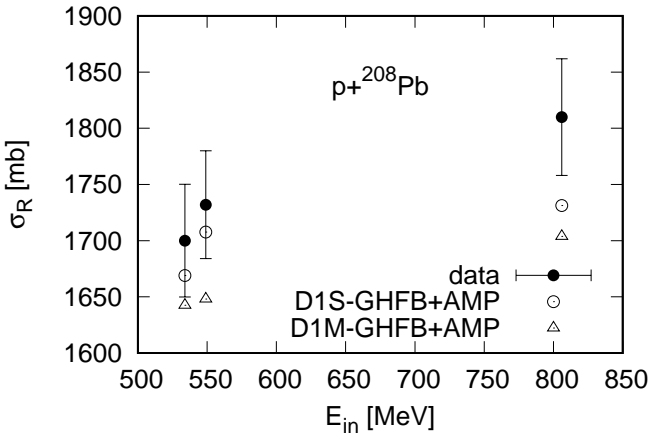


FIG. 1. E_{lab} dependence of reaction cross sections σ_R for $p + {}^{208}\text{Pb}$ scattering. Open circles stand for the results of the LF t -matrix folding model with the D1S-GHFB+AMP densities, whereas open triangles correspond to that with the D1M-GHFB+AMP densities. The data are taken from Refs. [23, 24].

Now we scale the D1S-GHFB+AMP neutron density so that the result of the LF t matrix folding model agrees with the data [23, 24]. In the present case, the neutron scaling factor is $\alpha = 1.017$. Since the resulting $r_n(\text{exp})$ depends on E_{lab} , we take the weighted mean and its total error for $E_{\text{lab}} = 534.1, 549, 806$ MeV. Neutron and matter radii thus obtained are $r_n(\text{exp}) = 5.768 \pm 0.047$ fm and $r_m(\text{exp}) = 5.643 \pm 0.047$ fm, leading to $r_{\text{skin}}^{208}(\text{exp}) = 0.324 \pm 0.047$ fm.

The same procedure is taken for D1M-GHFB+AMP. This leads to $r_{\text{skin}}^{208}(\text{exp}) = 0.333 \pm 0.047$ fm, where the neutron scaling factor is $\alpha = 1.038$. The theoretical error is evaluated with the difference between the central values of D1S-GHFB+AMP and D1M-GHFB+AMP. The value is 0.009 fm. The result of D1S-GHFB+AMP yields better agreement with the data than that of D1M-GHFB+AMP. We then obtain $r_{\text{skin}}^{208}(\text{exp}) = 0.324 \pm (0.047)_{\text{exp}} \pm (0.009)_{\text{th}}$ fm.

Discussions: Finally, the uncertainties of our results are listed.

1. Ambiguity of original densities taken:

As for proton and neutron densities for ${}^{48}\text{Ca}$, we used D1S and D1M in Ref. [38]. Our result is $r_{\text{skin}}^{48}(\text{exp}) = 0.158 \pm (0.023)_{\text{exp}} \pm (0.012)_{\text{th}}$ fm; the theoretical error $(0.012)_{\text{th}}$ fm is evaluated with D1S and D1M. The same procedure is taken for ${}^{208}\text{Pb}$. Our result is $r_{\text{skin}}^{208}(\text{exp}) = 0.324 \pm (0.047)_{\text{exp}} \pm (0.009)_{\text{th}}$ fm.

2. Experimental ambiguity:

Our present result $r_{\text{skin}}^{48} = 0.144 \pm 0.075$ fm based on Δ is consistent with $r_{\text{skin}}^{48}(\text{exp}) = 0.158 \pm (0.023)_{\text{exp}} \pm (0.012)_{\text{th}}$ fm of Ref. [38]. The central values are different from each other. The difference comes from the data used.

Conclusion: Our final values are $r_{\text{skin}}^{208}(\text{exp}) = 0.324 \pm (0.047)_{\text{exp}} \pm (0.009)_{\text{th}}$ fm and $r_{\text{skin}}^{48} = 0.144 \pm 0.075$ fm. Our values are consistent with r_{skin}^{208} (PREX2) and r_{skin}^{48} (CREX), respectively. These values are tabulated in Table I.

TABLE I. Results for $r_{\text{skin}}^{208}(\text{exp})$ and $r_{\text{skin}}^{48}(\text{exp})$. The values are shown in units of fm.

	$r_{\text{skin}}^{208}(\text{exp})$ or $r_{\text{skin}}^{48}(\text{exp})$
PREX2	0.283 ± 0.071
TW (${}^{208}\text{Pb}$)	$0.324 \pm (0.047)_{\text{exp}} \pm (0.009)_{\text{th}}$
CREX	$0.121 \pm 0.026(\text{exp}) \pm 0.024(\text{model})$
TW (${}^{48}\text{Ca}$)	0.144 ± 0.075

ACKNOWLEDGMENTS

We would like to thank Dr. Toyokawa from his contribution.

-
- [1] C. J. Horowitz, S. J. Pollock, P. A. Souder, and R. Michaels, Phys. Rev. C **63**, 025501 (2001).
- [2] D. Adhikari et al. (PREX), Phys. Rev. Lett. **126**, 172502 (2021), arXiv:2102.10767 [nucl-ex].
- [3] S. Abrahamyan, Z. Ahmed, H. Albataineh, K. Aniol, D. S. Armstrong, W. Armstrong, T. Averett, B. Babineau, A. Barbieri, V. Bellini, et al. (PREX Collaboration), Phys. Rev. Lett. **108**, 112502 (2012).
- [4] C. J. Horowitz, Z. Ahmed, C.-M. Jen, A. Rakhman, P. A. Souder, M. M. Dalton, N. Liyanage, K. D. Paschke, K. Saenboonruang, R. Silwal, G. B. Franklin, M. Friend, B. Quinn, K. S. Kumar, D. McNulty, L. Mercado, S. Riordan, J. Wexler, R. W. Michaels, and G. M. Urciuoli, Phys. Rev. C **85**, 032501 (2012).
- [5] D. Adhikari et al. (CREX), Phys. Rev. Lett. **129**, 042501 (2022), arXiv:2205.11593 [nucl-ex].
- [6] S. J. Novario, G. Hagen, G. R. Jansen, and T. Papenbrock, Phys. Rev. C **102**, 051303 (2020).
- [7] H. Shen, F. Ji, J. Hu, and K. Sumiyoshi, Astrophys. J. **891**, 148 (2020).
- [8] C. Horowitz, Ann. Phys. (Amsterdam) **411**, 167992 (2019).
- [9] Wei, Jin-Biao, Lu, Jia-Jing, Burgio, G. F., Li, Zeng-Hua, and Schulze, H.-J., Eur. Phys. J. A **56**, 63 (2020).
- [10] M. Thiel, C. Sfienti, J. Piekarwicz, C. J. Horowitz, and M. Vanderhaeghen, J. Phys. G: Nucl. Part. Phys. **46**, 093003 (2019).
- [11] B. T. Reed, F. J. Fattoyev, C. J. Horowitz, and J. Piekarwicz, arXiv:2101.03193 [nucl-th].
- [12] A. Trzcińska, J. Jastrzębski, P. Lubiński, F. J. Hartmann, R. Schmidt, T. von Egidy, and B. Kłos,

- Phys. Rev. Lett. **87**, 082501 (2001).
- [13] J. Zenihiro, H. Sakaguchi, T. Murakami, M. Yosoi, Y. Yasuda, S. Terashima, Y. Iwao, et al., Phys. Rev. C **82**, 044611 (2010).
- [14] A. Tamii, I. Poltoratska, P. von Neumann-Cosel, Y. Fujita, T. Adachi, C. A. Bertulani, J. Carter, et al., Phys. Rev. Lett. **107**, 062502 (2011).
- [15] C. M. Tarbert, D. P. Watts, D. I. Glazier, P. Aguar, J. Ahrens, J. R. M. Annand, H. J. Arends, R. Beck, V. Bekrenev, B. Boillat, et al. (Crystal Ball at MAMI and A2 Collaboration), Phys. Rev. Lett. **112**, 242502 (2014).
- [16] M. C. Atkinson, M. H. Mahzoon, M. A. Keim, B. A. Borodelon, C. D. Pruitt, R. J. Charity, and W. H. Dickhoff, Phys. Rev. C **101**, 044303 (2020).
- [17] S. Tagami, T. Wakasa, J. Matsui, M. Yahiro, and M. Takechi, Phys. Rev. C **104**, 024606 (2021), arXiv:2010.02450 [nucl-th].
- [18] M. Matsuzaki, S. Tagami, and M. Yahiro, Phys. Rev. C **104**, 054613 (2021), arXiv:2107.06441 [nucl-th].
- [19] S. Tagami, M. Tanaka, M. Takechi, M. Fukuda, and M. Yahiro, Phys. Rev. C **101**, 014620 (2020).
- [20] W. G. Love and M. A. Franey, Phys. Rev. C **24**, 1073 (1981).
- [21] A. B. Jones and B. A. Brown, Phys. Rev. C **90**, 067304 (2014).
- [22] T. Wakasa, S. Tagami, J. Matsui, M. Yahiro, and M. Takechi, Results in Physics **29**, 104749 (2021).
- [23] F. S. Dietrich et al., J. Nucl. Sci. Tech. **39**, 269 (2002).
- [24] M. Nakano, Y. Yamaguchi, and Y. Uozumi, Phys. Rev. C **103**, 044608 (2021).
- [25] J. Birkhan et al., Phys. Rev. Lett. **118**, 252501 (2017), arXiv:1611.07072 [nucl-ex].
- [26] J. Zenihiro et al., (2018), arXiv:1810.11796 [nucl-ex].
- [27] I. Angeli and K. Marinova, At. Data Nucl. Data Tables **99**, 69 (2013).
- [28] S. R. Neumaier et al., Nucl. Phys. A **712**, 247 (2002).
- [29] T. Wakasa, M. Takechi, S. Tagami, and M. Yahiro, Results in Physics , 105329 (2022).
- [30] F. A. Brieva and J. R. Rook, Nucl. Phys. **291**, 299 (1977).
- [31] F. A. Brieva and J. R. Rook, Nucl. Phys. **291**, 317 (1977).
- [32] F. A. Brieva and J. R. Rook, Nucl. Phys. **297**, 206 (1978).
- [33] K. Minomo, K. Ogata, M. Kohno, Y. R. Shimizu, and M. Yahiro, J. Phys. G **37**, 085011 (2010), arXiv:0911.1184 [nucl-th].
- [34] S. Tagami, M. Tanaka, M. Takechi, M. Fukuda, and M. Yahiro, Phys. Rev. C **101**, 014620 (2020), arXiv:1911.05417 [nucl-th].
- [35] T. Sumi, K. Minomo, S. Tagami, M. Kimura, T. Matsumoto, K. Ogata, Y. R. Shimizu, and M. Yahiro, Phys. Rev. C **85**, 064613 (2012), arXiv:1201.2497 [nucl-th].
- [36] S. Goriely, S. Hilaire, M. Girod, and S. Peru, Phys. Rev. Lett. **102**, 242501 (2009).
- [37] L. M. Robledo, T. R. Rodríguez, and R. R. Rodríguez-Guzmán, J. Phys. G **46**, 013001 (2019), arXiv:1807.02518 [nucl-th].
- [38] S. Tagami, T. Wakasa, M. Takechi, J. Matsui, and M. Yahiro, Results in Physics **33**, 105155 (2022).